CHAPTER 4 – LiDAR APPLICATIONS TO ROCK SLOPES

This chapter provides details on how LiDAR can be used to assist with highway rock slope stability analyses. This chapter is separated into the three sections: rock mass characterization, rockfall characterization, and detailed 3D measurements.

ROCK MASS CHARACTERIZATION

As described in Chapter 1, rock mass characterization is the process of obtaining data for rock slope stability, and in the current practice much of this information is obtained by hand at highway slopes and natural rock outcrops. This section describes the use of LiDAR (and associated digital images) to obtain this information. At the present time, rock mass information that is being obtained from LiDAR includes discontinuity orientation, length, spacing, roughness, and block size (Kemeny et al., 2006a, 2006b, 2006c). In addition, research is presently being conducted to obtain additional information, including geology, weathering and discontinuity fill (Kemeny, 2006b).

Discontinuity Orientation

Figure 4 illustrates the general procedure used to obtain information on discontinuity orientation. The first step is to scan a field site of interest, produce a point cloud, and register the scan into a terrestrial coordinate system (as described in Chapter 2). Figure 4a shows a field site in Colorado that was scanned using an Optech ILRIS 3D scanner, and Figure 4b shows the point cloud from this site. The next step is to create a surface mesh from the point cloud data. In the process of creating a surface mesh, erroneous data points in the point cloud can be filtered. This includes the removal of points outside the area of interest, the removal of points directly in front of the area of interest (due to cars, dust or other objects causing an erroneous laser reflection), and the removal of non-rock objects on the rock slope. The first two items are easily accomplished using standard hand-editing features in point cloud processing software. The third item is more difficult and requires either significant hand-editing or the development of special vegetation or other types of filters (Virtual Geomatics, 2008; Pfeifer, 2004). Figure 4c shows a triangulated mesh of part of the point cloud shown in Figure 4b.

The most important processing step is the delineation of fracture “patches” from the triangulated surface mesh. The term “patch” is used rather than fracture, because a single large fracture may be delineated into several smaller patches, depending on the flatness and roughness of the fracture. Fractures are detected by using the basic property that they are flat. Flat surfaces are automatically found in the triangulated mesh by first calculating the normal to each triangle, and then finding groups of adjacent triangles that satisfy a flatness criterion. This criterion has parameters that can be adjusted by the user.

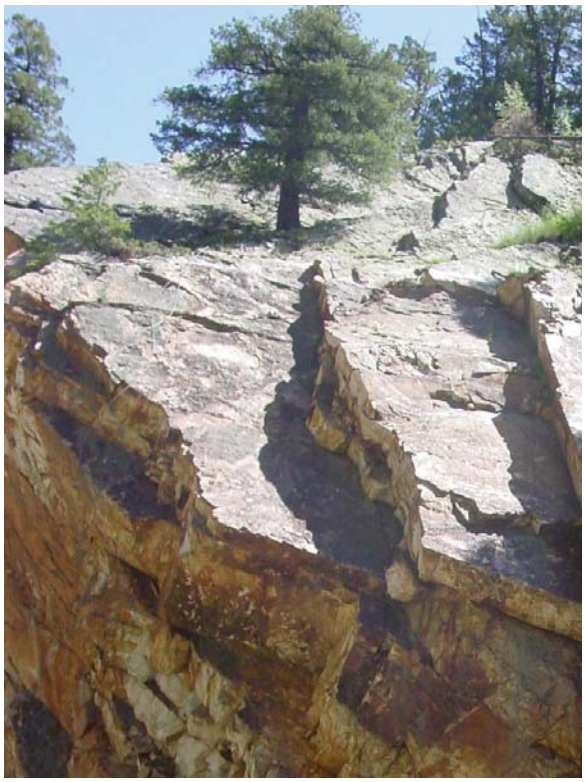

Figure 4a. Photo. Field site that was scanned using ground-based LiDAR.

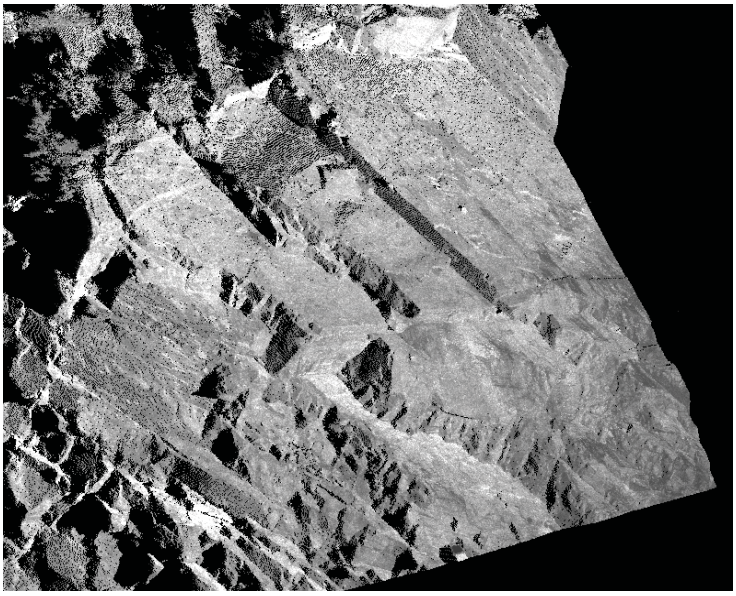

Figure 4b. Schematic. Point cloud for the field site shown in Figure 4a.

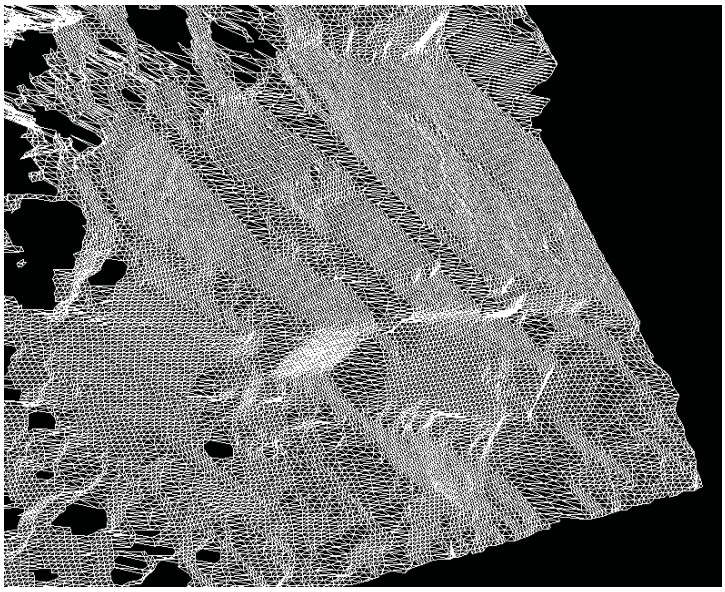

Figure 4c. Schematic. Triangulated mesh for point cloud shown in Figure 4b.

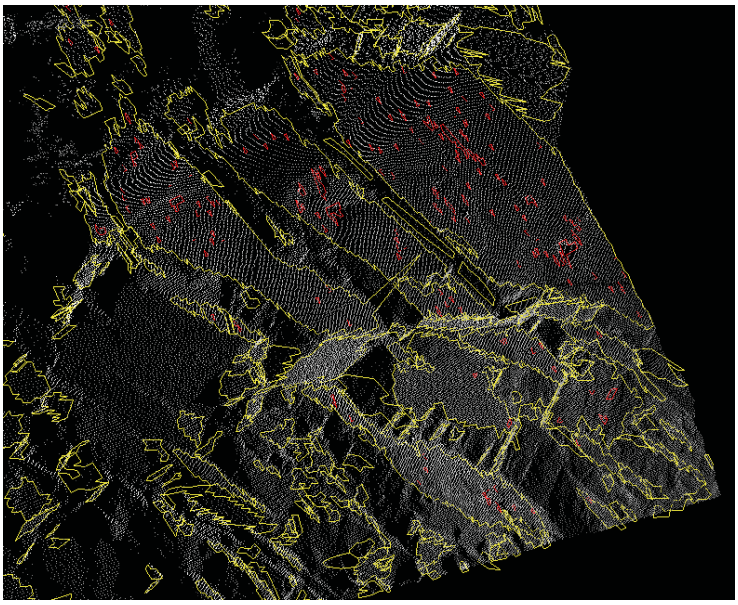

Figure 4d. Schematic. Automatic delineation of fractures for the point cloud in Figure 4b.

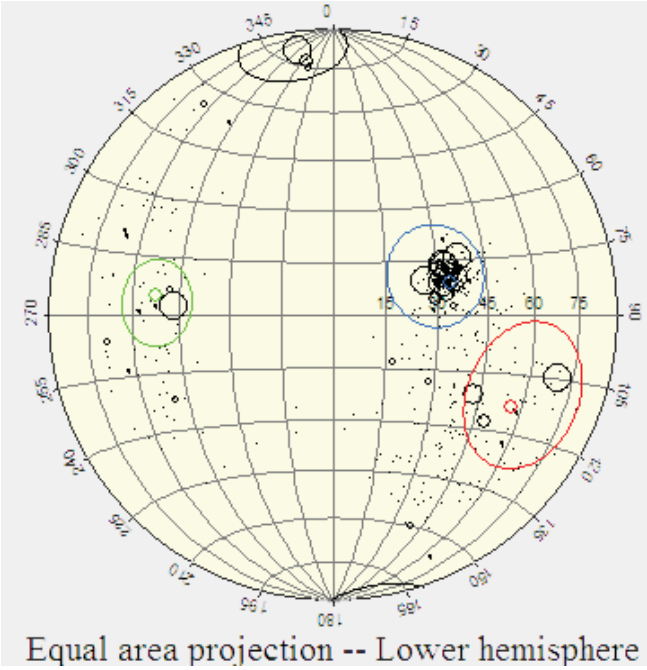

Figure 4e. Plot. Stereonet plot of fractures from Figure 4d.

Figure 4d shows the patches that were found in the point cloud shown in Figure 4b, using the criterion that a patch must be at least 5 triangles, and neighboring triangles in a patch must not deviate in orientation by more than 10 degrees. The patches are outlined in yellow and holes in patches are outlined in red. Overall this simple criterion results in a good delineation of the major fractures at the site. Patches can also be manually added, deleted and edited. Once the patches have been found, their average orientations can be plotted on a stereonet. Each patch plots as one point on the stereonet. However the size of the point can be adjusted based on other parameters such as the patch area or roughness. Large patches are a good indication of important fractures and fracture sets. Small patches, on the other hand, may not actually be a fracture but only a small portion of the surface that happens to be flat. Thus it is useful to weight the points by fracture area, and plot the smallest fractures as only a small dot. Figure 4e is a plot of the patches from Figure 4d, weighted by patch area. Four fracture sets can be clearly seen and have been outlined in Figure 4e. Once the sets are identified, the statistical properties of each set can be determined. The total time spent to produce the results shown in Figure 3 from the previous chapter, starting from the raw point cloud file, is less than one hour.

A particularly useful feature of point cloud processing software is the interaction it allows between the stereonet and the point cloud. Delineating joint sets from stereonet data is difficult and necessitates professional expertise. Normally the data is taken in the field and the compilation and definition of joint sets is accomplished at a later time. Therefore, any difficulties with interpretation of the data cannot be resolved without additional field work. With access to the point cloud, however, additional analysis can easily be conducted off site. For instance, a group of patches can be selected on the stereonet and then viewed on the point cloud. This allows the user to go back and forth between the stereonet and the point cloud to determine with a great deal of precision the delineation of important fractures and fracture sets.

Figure 5 shows an example from a highway slope near milepost 8 along the Mt. Lemmon Highway near Tucson, Arizona. In this case a single scan was made, and scanner registration consisted of Brunton measurements of the scanner position. Automatic fracture delineation was conducted and the results are shown in the black stereonet in Figure 5 (over 1000 data points). Fractures with different orientations are shown with different colors, which assists with interpreting the structure (Jaboyedoff et al., 2007). In Figure 5 the results are also compared with traditional, manually-collected scanline mapping (white stereonet with 50 measurements). The results show that there is a very good correlation between the manual and LiDAR-generated data. The man-hours needed to produce the stereonets can also be compared. Traditional scanline mapping at this site required about 5 hours, which consisted of manual measurements in the field (4 hours), data entry into the computer (30 minutes) and stereonet plotting (30 minutes).

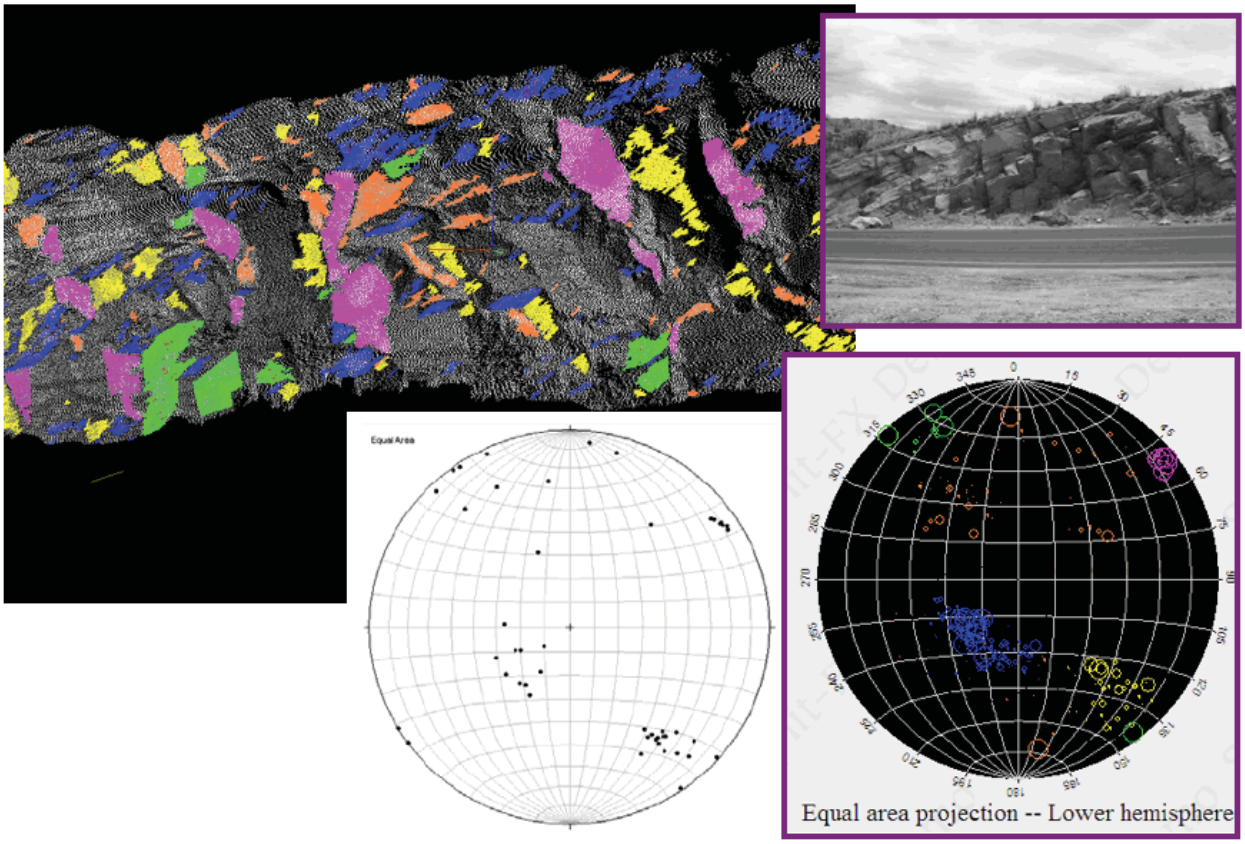

Figure 5. Photo and Schematic. Scan on Mt. Lemmon Highway. Comparison of LiDAR generated data (black stereonet) with hand measurements (white stereonet).

The LiDAR generated data required less than 2 hours, which consisted of scanner setup in the field and Brunton measurements of the scanner orientation (30 minutes), scanning (15 minutes), downloading data from the scanner to the computer (15 minutes), and processing the point cloud data in the Split FX program (45 minutes). Not only did the LiDAR scanning require less time, but 20 times more fracture poles were generated from LiDAR than in the traditional scanline mapping (1000 LiDAR generated poles vs. 50 manual). In several cases, a discontinuity set is represented by a single measurement in the manual measurements (which would undoubtedly be thrown out in the any analyses), compared with a large number of poles in the LiDAR-generated data. The shapes of the fracture sets are also much better defined in the LiDAR generated data

because of the large number of data points. In some cases, particularly slopes where access is very difficult, the LiDAR generated data could represent a cost savings over traditional measurements. This is discussed in more detail at the end of this chapter.

The number of laser points that strike a fracture surface will depend on many factors, including the laser resolution, the size of the fracture, the distance of the fracture, and the orientation of the fracture relative to the scanner orientation. Fractures that are sub-parallel to the direction of scanning may be under-represented on the stereonet because fewer laser points will strike those surfaces. However, a careful evaluation of the point cloud and the stereonet can reveal those under-represented areas in the stereonet, and patches can be added accordingly using hand-editing tools in the point cloud processing software. The scanner can only detect surfaces that are in the scanner's line of sight, and the portion of the surface that is not in the scanner's line of site is referred to as the scanner "shadow zone". In some circumstances, an entire joint set may be in the scanner shadow zone, and in these cases several scans need to be taken at different angles to the face in order to adequately represent the structural conditions at the site.

If a structural feature (such as a joint set) is in the shadow zone, it is likely that traces of the structure will still be visible from the direction the scan was taken, and in these cases photo draping can be used to extract the orientation of the structure. Details on photo draping (also called texture mapping) are described in Blythe (1999). An example of photo draping is shown in Figure 6. Figures 6a and 6b demonstrate the draping of a high-resolution digital image over the point cloud for the outcrop shown in Figure 5. Three "pins" were used to align the photo over the point cloud. The pins are first inserted into the digital image at specific locations (red dots in Figure 6a), and then on the point cloud the pins are moved to the same locations (red dots in Figure 6b). Figure 6c shows a location where six traces were made on the digital image. In one case the trace was made of a fracture that showed relief so that the orientation could be determined from both the trace and the point cloud. In the other five cases, the orientation could not be determined from the point cloud. Figure 6d shows the extracted 3D orientations from the traces. Photo-draping works well in extracting 3D orientations from traces, and in studies where both traces and fracture surfaces were available, the orientation results from draping agree within a few degrees with the point cloud results.

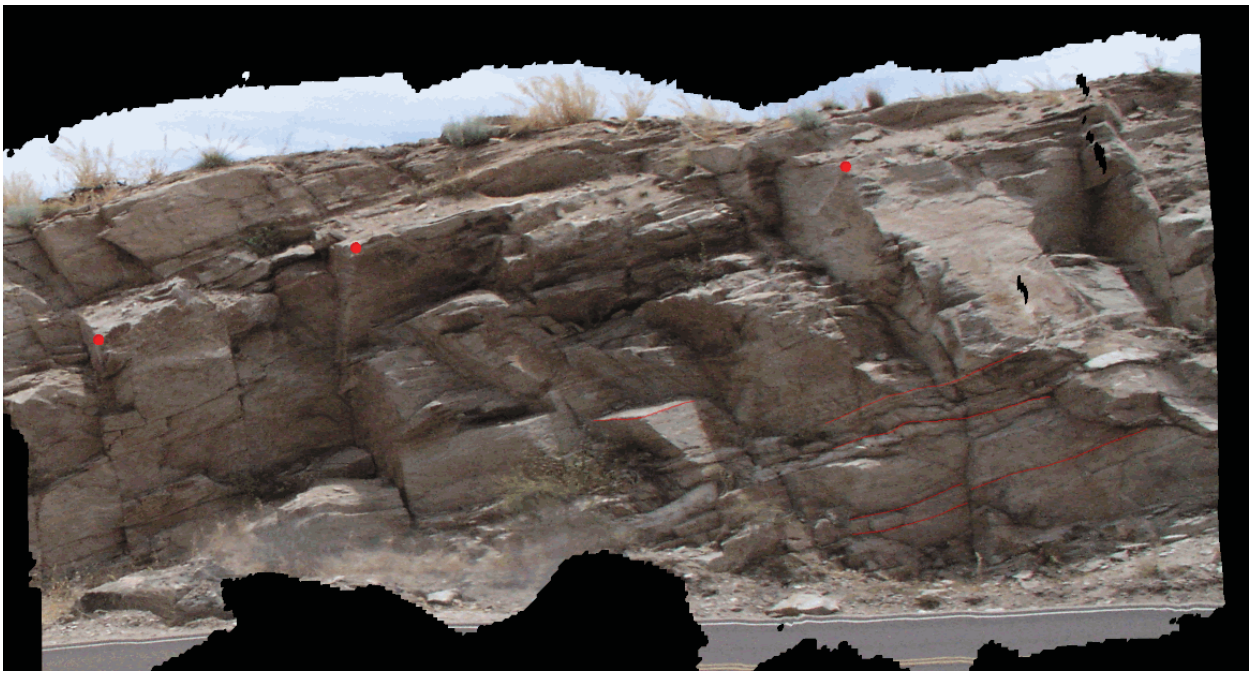

Figure 6a. Photo. Step 1 in photo draping procedure, insert pins on digital image.

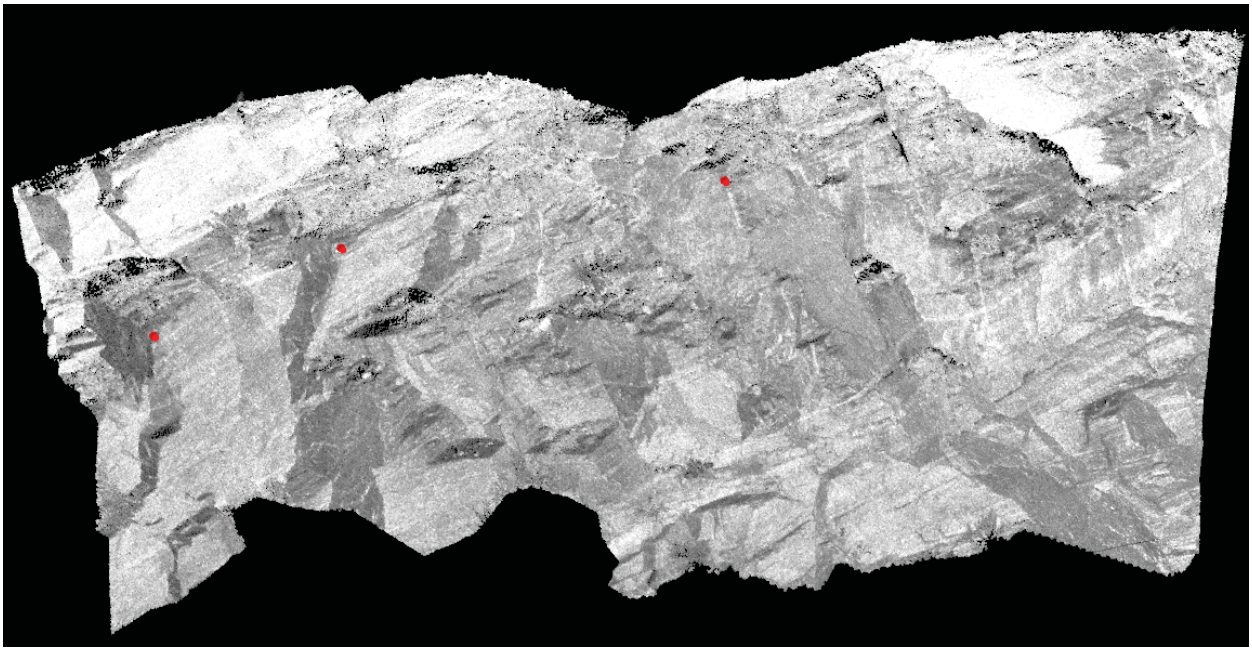

Figure 6b. Photo. Step 2 in photo draping procedure, align pins on point cloud to the same position as in digital image.

Figure 6c. Photo. Step 3 in photo draping procedure, delineate fracture traces on the digital image.

Figure 6d. Photo. Step 4 in photo draping procedure, three dimensional fracture orientations extracted from the traces.

The procedure described above can also be used to determine the orientation of a single critical structure such as a fault. A fault can be more clearly identified on the digital image rather than the point cloud. Also, because a fault is weak, it may not show any three dimensional surfaces where the orientation could be extracted from the point cloud alone. In this case the fault can be traced on the digital image and the orientation determined from the technique described above.

Discontinuity Roughness

There are several ways that LiDAR data can be used to get information on discontinuity roughness. The first way is to use a triangulated mesh of a fracture, as illustrated in Figure 7. If the orientation of each triangle is plotted on a stereonet, then the scatter about the mean orientation of the fracture gives information on the dilatation angle. In the classic saw-toothed fracture analyzed by Patton (1966), the dilatation angle is defined as the rise angle of the saw teeth compared with the mean orientation, as shown in Figure 7. The dilatation angle is directly related to the additional friction angle due to roughness (Goodman, 1989), and on a stereonet, the dilatation angle can be directly determined by the angle between the mesh triangle orientation and the mean orientation of the fracture. The example in Figure 7 shows a scatter of triangle orientations, with the mean fracture orientation at the center of the scatter. The stereonet in Figure 7 is marked off in degree increments of 10 degrees, and indicates dilatation angles ranging from a few degrees to over 30 degrees. Also the shape of the scatter in the stereonet is elliptical, indicating roughness anisotropy (dilatation angle varies with direction). By varying the triangle size of the mesh, scale-dependent roughness can be determined. As an important note, the triangle size needs to be greater than the scanner error, or else roughness due to measurement error will be calculated. For example, in Figure 7 the triangle size was about 8 cm, compared to the point spacing of about 1 cm and scanner error of about 0.5 cm.

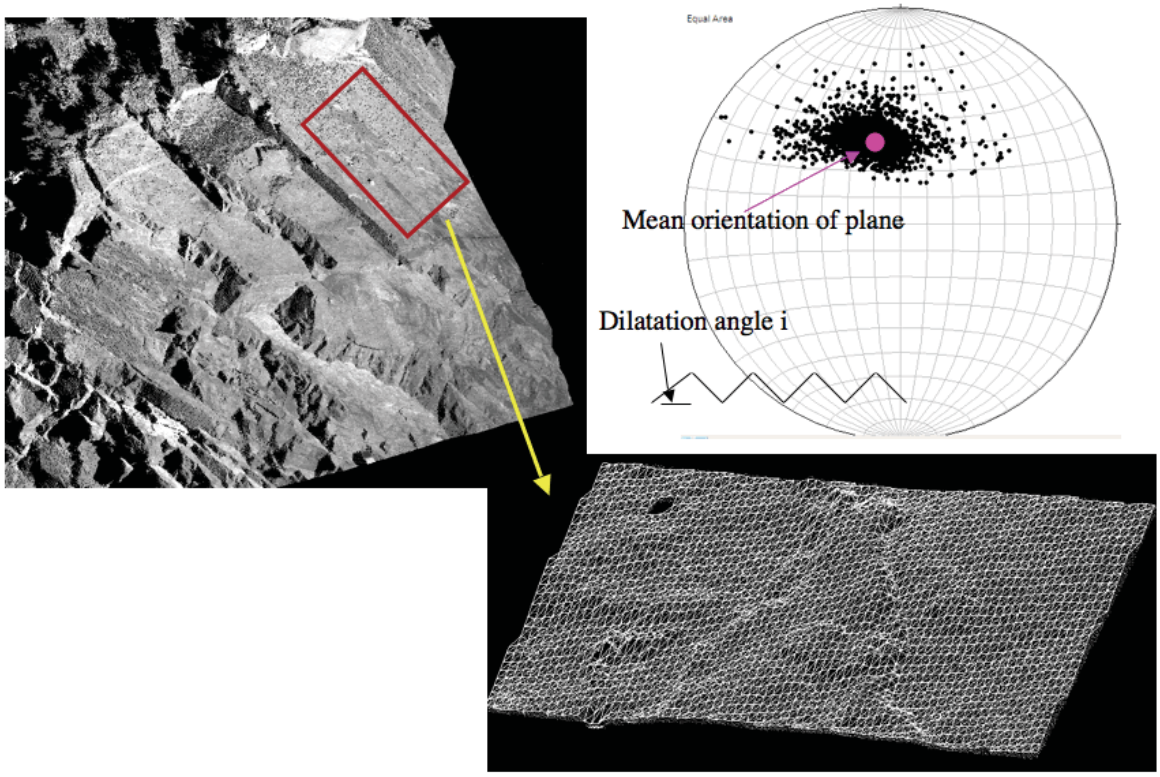

Figure 7. Schematics. One method of analyzing fracture roughness using LiDAR data, by making a triangulated mesh of a fracture and plotting the pole for each triangle on a stereonet.

Figure 8 gives a second example taken from the scan of an open pit mine in Montana. Two large fractures shown in Figure 8 have been analyzed using the technique described above, and the triangle orientations are presented in contoured stereonets in Figures 8b and 8c. Eliminating the outlier triangles and considering the contour representing about 90% of the poles (lightest blue contour), maximum dilatation angles of 10-15 degrees are revealed.

Figure 8a. Photo. Location of two large fractures for determination of maximum dilatation angle using the method described in Figure 7.

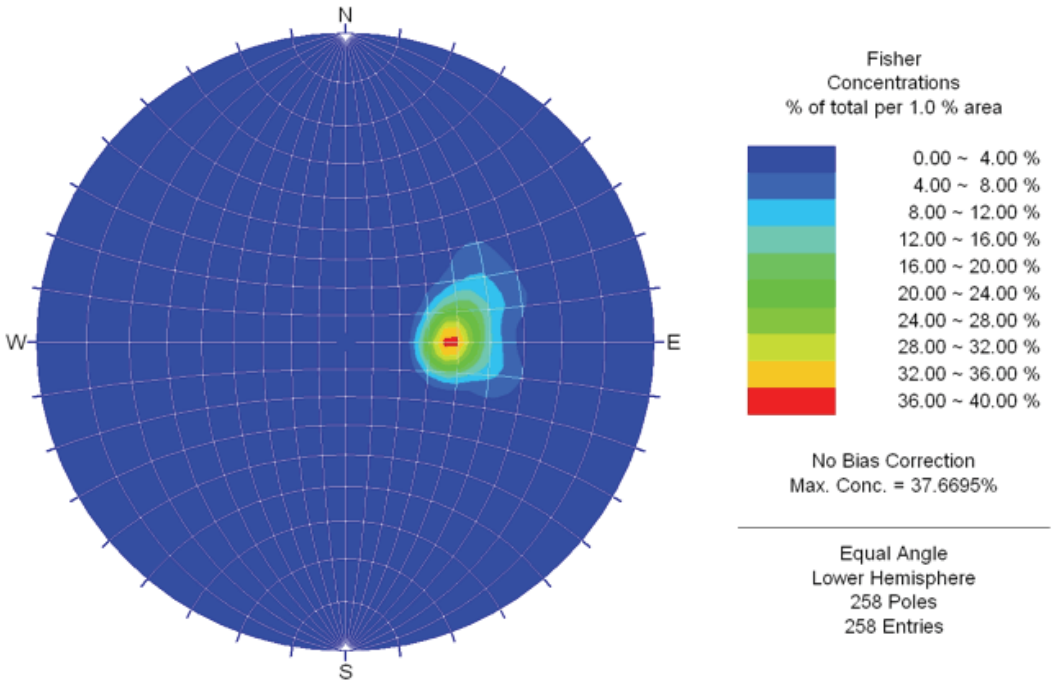

Figure 8b. Chart. Contoured stereonet of poles of each mesh triangle in left fracture shown in Figure 8a.

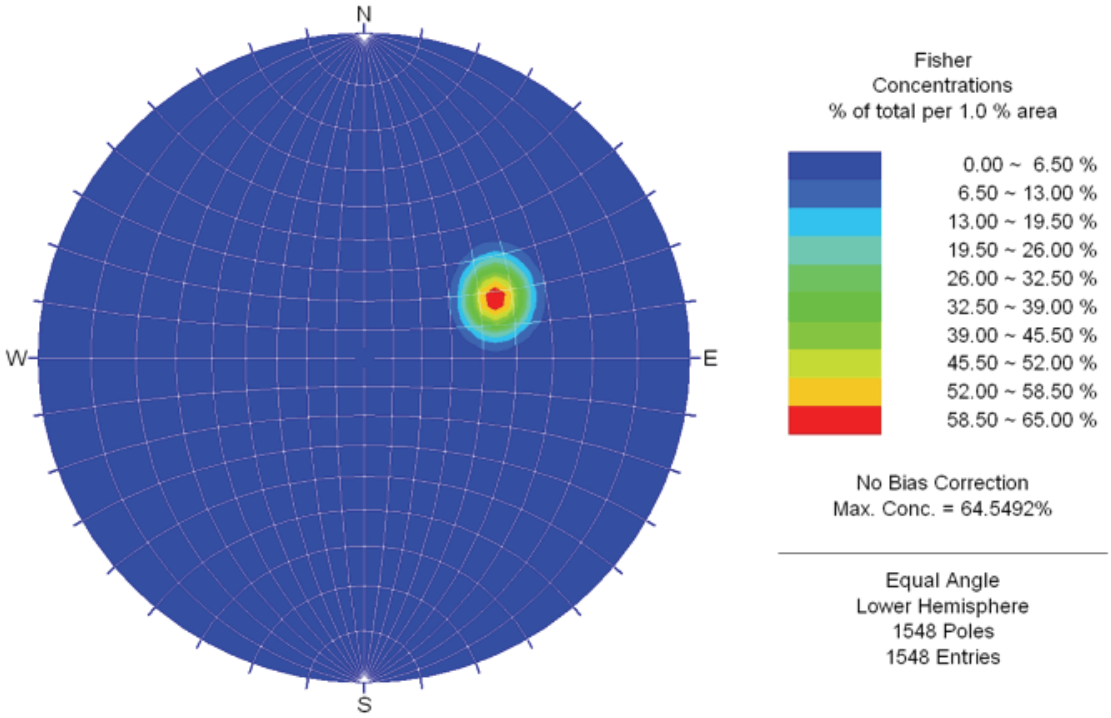

Figure 8c. Chart. Contoured stereonet of poles of each mesh triangle in right fracture shown in Figure 8a.

The second way to get information about roughness is to make cross sections through a fracture at different angles (a cross section in the direction of the dip vector, for instance, would be relevant for slope stability purposes). Figure 9 illustrates the procedure. The roughness profiles are calculated from the triangulated surface, and therefore the same aforementioned scale-dependence and caution about noise are applicable. There are several published methods for extracting fracture roughness information from two dimensional roughness profiles. For instance, Tse and Cruden (1979) describe a technique where Z_2, the root mean square of the derivative of the profile, is first calculated. The Joint Roughness Coefficient (JRC, see Hoek, 2007) is then calculated using the empirical formula:

$$JRC = 32.2 + 32.47 \log Z_2. \quad (3)$$

This technique was used successfully by Haneberg (2007). Studies with this technique have shown that it can sometimes give values of JRC outside the range of 0-20, and therefore the technique described in Figures 7 and 8 is preferred at this time.

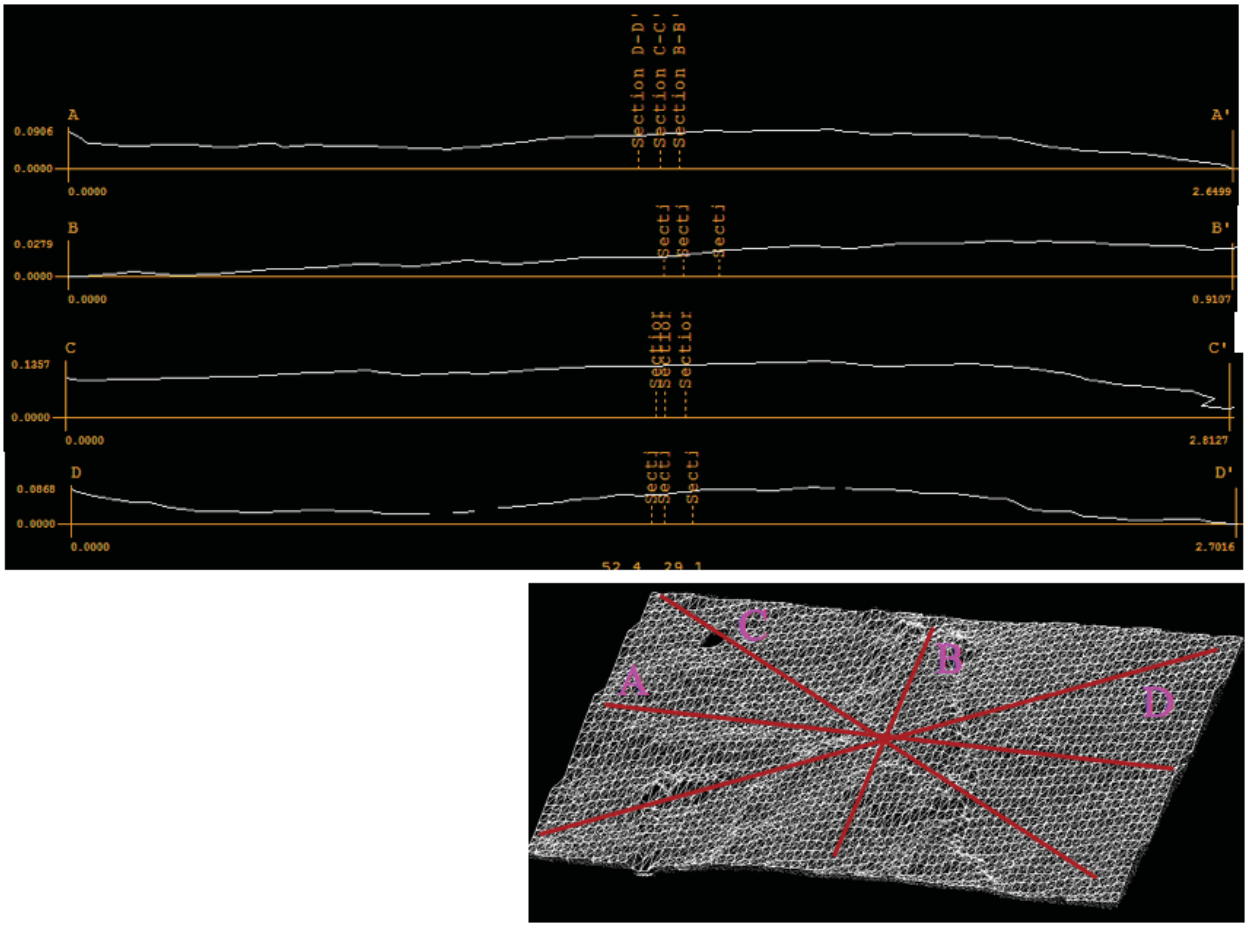

Figure 9. Schematic. A second method of analyzing fracture roughness, by making topographic profiles of the fracture in different directions, and processing the roughness profile to extract roughness parameters such as JRC.

Fracture Length and Spacing

Fracture length and spacing can be measured from either digital images or point clouds, as shown in Figure 10. In two dimensions (measured from a digital image of a road cut, for instance), the measured fracture spacing is referred to as the "apparent" spacing, and can be corrected if the true average orientation of the set is known. In three dimensions (measured from a point cloud or a draped photo), the true spacing can be measured directly if the measurement is made perpendicular to the average strike of the set.

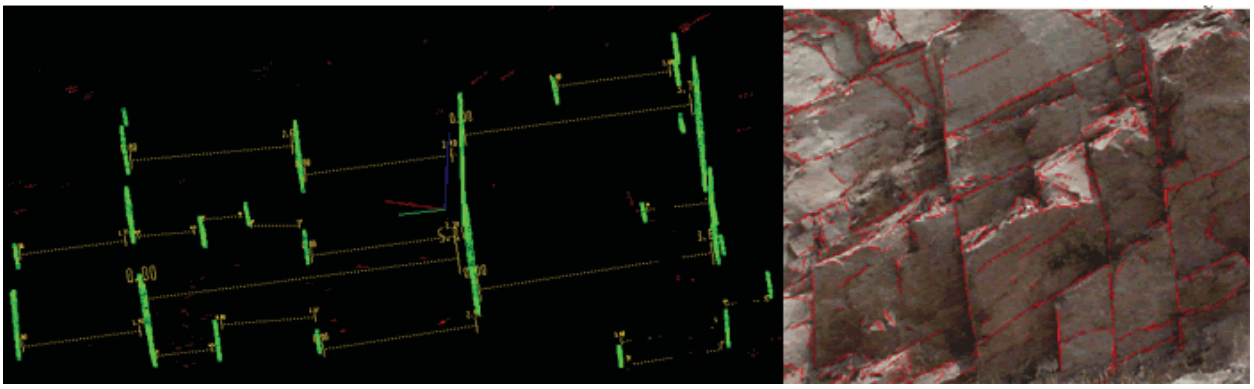

a) b)

Figure 10. Photo and Schematic. Information on fracture length and spacing can be extracted from both a) point clouds, and b) digital images.

Automatic trace delineation involves image processing algorithms called edge detectors (Gonzalez and Wintz, 1987). The development of edge detection algorithms for rock fractures are described in Hadjigeorgiou et al. (2003), Kemeny and Post (2003) and others. Even though automatic trace delineation algorithms are available in many image-processing programs (including Split FX), they are not recommended at this time for several reasons. First of all, they will delineate all the fractures in an image, which will undoubtedly come from several structural sets (as illustrate in Figure 10b). This means that in order to determine statistical parameters for each set, hand editing will still be necessary. Secondly, due to the complexity of images of rock outcrops, no automatic routine will do a perfect job of delineation and corrections will need to be made using hand editing tools. Thirdly, it does not take very long and does not require expertise to delineate fractures by hand. The traces in Figure 10b, for instance, took only several minutes to delineate.

Fracture length and spacing are interrelated, as illustrated in Figure 11. If the fractures are persistent (fractures long in relation to the spacing), then the measurement of fracture spacing for a given set is well defined and measured perpendicular to the average orientation of the set, as illustrated by the red "scanline" in Figure 11a. If the fractures are non-persistent (fractures short in relation to spacing), then the measurement of fracture spacing is not well defined by a single scanline, and several scanlines perpendicular the average orientation are needed, as illustrated by the green scanlines in Figure 11b. In either case, a histogram of fracture spacing is produced for each set.

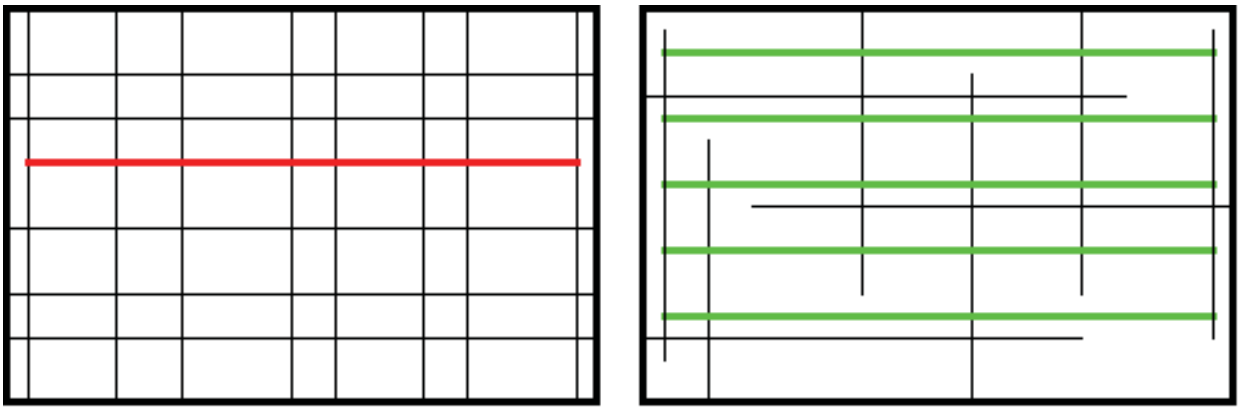

a) b)

Figure 11. Schematic. Persistent vs. non-persistent discontinuities (black lines). a) persistent discontinuities, with a single scanline (red) to obtain fracture spacing information, b) non-persistent discontinuities, with multiple scanlines (green) used to obtain fracture spacing information.

In order to get accurate information on fracture length and spacing from digital images, proper images must be taken. Figure 12 shows two digital images of rock outcrops. In the first image the joint traces are clear and the scale of the image is appropriate for the density of joints. In the second image, the individual joint traces are difficult to see because the scale of the image is not appropriate for the density of joints at this site (close-up image needed to provide appropriate level of detail).

a) b)

Figure 12. Photos. a) digital image with the proper density of fracture information, b) figure cannot be analyzed at its current scale (close-up image needed to provide appropriate level of detail).

Block Size

Block size is a parameter that depends on the interaction of all the joint sets together, into a fracture network. In a similar fashion to fracture length and spacing, block size can be measured

from either a digital image or a point cloud, and either manually or using edge detection algorithms.

Figure 13 illustrates block delineation using manual tools for both digital images and point clouds. In the case of a digital image, the block area is calculated and the area must be converted to volume using an assumed length in the third dimension. In the case of the point cloud, the block volume is measured directly.

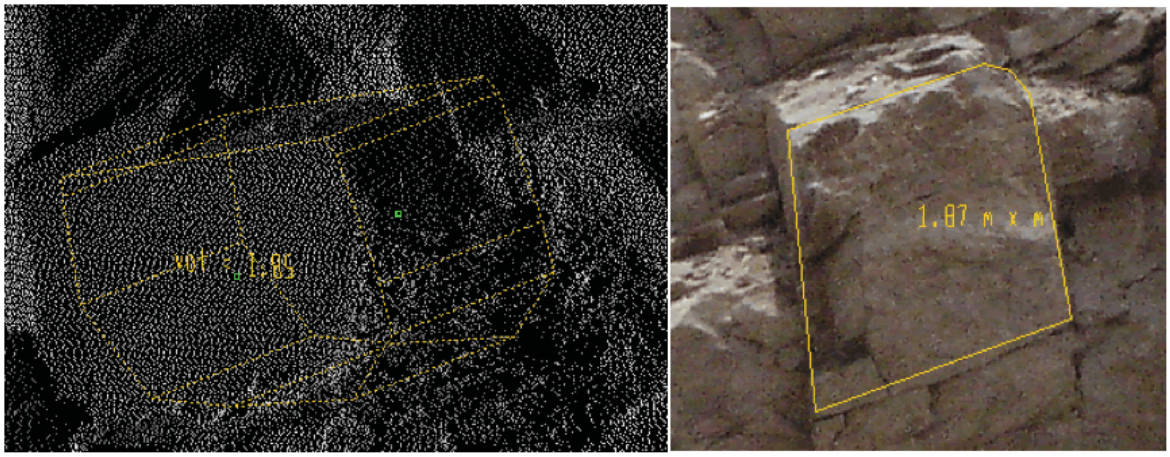

a) b)

Figure 13. Photos. Manual methods of getting block size information, both from a) point cloud and from b) digital image.

In order to automatically delineate blocks and determine the distribution of block volumes at a site, the rock bridges must be first identified. Rock bridges are small sections of intact rock that separate coplanar or non-coplanar discontinuities, and prevent blocks from being "removable". Similar to the problem of trace delineation, the identification of rock bridges in a digital image of a rock outcrop is not a simple problem, and the use of hand-editing tools, such as those shown in Figure 13, is recommended at the present time.

Discontinuity Weathering and Fill

All of the discontinuity parameters described above (orientation, length and spacing, roughness, block size) relate to the geometry of the discontinuities and the fracture network, and it has been demonstrated that LiDAR and digital image processing do an excellent job of providing information on these parameters. Equally important, however, is the "condition" of the discontinuities, which include parameters such as weathering and fill. These parameters directly relate to the friction angle of the discontinuities, and highly weathered fractures or fractures containing very weak fill can have dangerously low friction angles. Also, weathering and fill make up a large component of rock mass classification systems. For instance, in the Rock Mass Rating (RMR, Bieniawski, 1989), Q (Barton et al., 1974), and Geologic Strength Index (GSI, Hoek, 2007) systems, weathering and fill account for about 12%, 25%, and 30% of the total rating, respectively.

LiDAR and digital image processing have the potential for providing information on discontinuity weathering and fill, and this is an area of current research. Some initial work on using texture algorithms to evaluate discontinuity weathering was investigated by Monte (2004). A comparison of the texture of a weathered and unweathered fracture is shown in Figure 14. Monte (2004) found that texture algorithms at a given site were able to differentiate discontinuities with different amounts of weathering after the parameters in the algorithms were properly adjusted. However, these parameters had to be readjusted for other locations and other rock types.

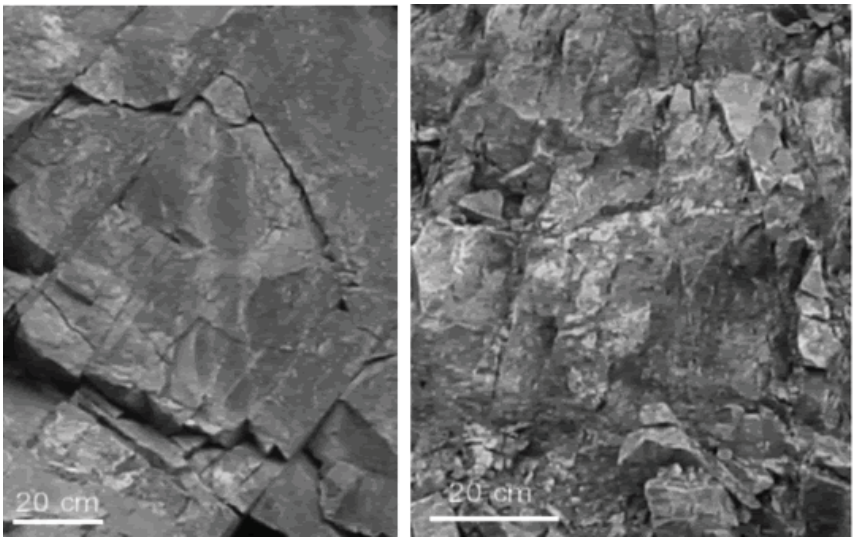

a) b)

Figure 14. Photos. Example of digital images of a) unweathered, and b) weathered discontinuities.

A more promising approach that is currently being investigated is using multi-spectral and hyper-spectral imaging to differentiate weathering and fill (Gupta et al., 1999). In particular, in many rock types weathering and fill is associated with clays, which can be identified with multi-spectral and hyper-spectral imaging. Determining the degree of weathering at a site at the present time is subjective because it is based primarily on visual inspection. However, the use of new techniques such as hyperspectral imaging could lead to more deterministic measures of weathering and discontinuity fill.

ROCKFALL CHARACTERIZATION

A second major highway application for LiDAR is rockfall characterization. This includes the characterization of rockfall source areas, the characterization of rockfall chutes, and monitoring rockfall occurrences by taking periodic scans of an area of interest.

Characterizing Rockfall Source Areas

Rockfall source areas can be characterized with LiDAR scans, to determine the risk for rockfall and slope instability. Characterization can include standard rock mass characterization as well as

rockfall hazard ratings (e.g., Patterson et al., 2002). Rockfall source areas are often difficult to access and characterize using traditional methods. Figure 15 shows before and after pictures of the source area for the 2004 Thanksgiving day rockfall that occurred along Interstate 70 in Glenwood Canyon, just east of Glenwood, CO. It was a large volume rockfall and the source area was on the north side of the canyon about 400 m (1312 ft) above the highway. Traditional site characterization in steep remote areas such as this involve rappeling down the slope, which is costly and poses safety hazards. The LiDAR techniques described earlier in this chapter are ideal for characterizing rockfall source areas.

Another example of a potential use of LiDAR for rockfall characterization is shown in Figure 16. It shows a highway slope near Pine Valley, California that is weathering and exposing large boulders that pose a rockfall hazard. LiDAR scanning of this slope could be used to determine the number and sizes of the boulders. Repeated scans at this same site over time could also be used to monitor the weathering process.

a) b)

Figure 15. Photos. Section of Glenwood Canyon a) before, and b) after the 2004 Thanksgiving Day rockfall.

Figure 16. Photo. Weathering of a slope near Pine Valley, California, exposing boulders that pose a rockfall hazard.

Rockfall Chutes

The rockfall source area determines the size and initial location of rock blocks that could impact a highway. When a rock block dislodges from a source area, it often travels along a developed path or chute until it reaches the highway. Therefore, the characteristics of rockfall chutes often determine the location, velocity and other aspects of a rockfall event. In particular, the chute characteristics must be understood in order to design rockfall fences or other support measures. One important aspect of the rockfall chute is the topographic profile, which can be characterized with LiDAR using cross section tools. Figure 17 shows photos and profiles of a major rockfall chute on the north side of Interstate 70 near Georgetown, Colorado (scan taken from the Georgetown Interstate 70 overlook). Figure 17a shows a photo of the scan area, with the rockfall source area at the top of the photo, the chute in the middle and rockfall fences near the bottom of the photo. Figure 17b shows a side view of the point cloud, showing the scanner, scanner direction and Interstate 70 at the bottom right, and the rockfall source area at the upper left (horizontal scale reads 460 m, vertical scale reads 328 m). The rockfall source area is about 600 meters (1969 ft) from the scanner. Figure 17c is a plan view of the point cloud showing two cross-sections through the chute area; one to the right of the trees down the middle of the chute (Section A) and the other to the left of the trees (Section B). Figures 17d and 17e show the profiles from sections A and B, respectively. The sections are made through the triangulated mesh, and gaps in the sections are areas where the mesh was not constructed due to insufficient point cloud data). The two profiles are similar except for the steep section in the center of section A, due to a small rock outcrop that can be seen in the close up photo in Figure 17f. Figure 17g shows close ups of the point cloud near the rockfall fences.

Figure 17a. Photo. Rockfall chute, north side of Interstate 70 near Georgetown, Colorado.

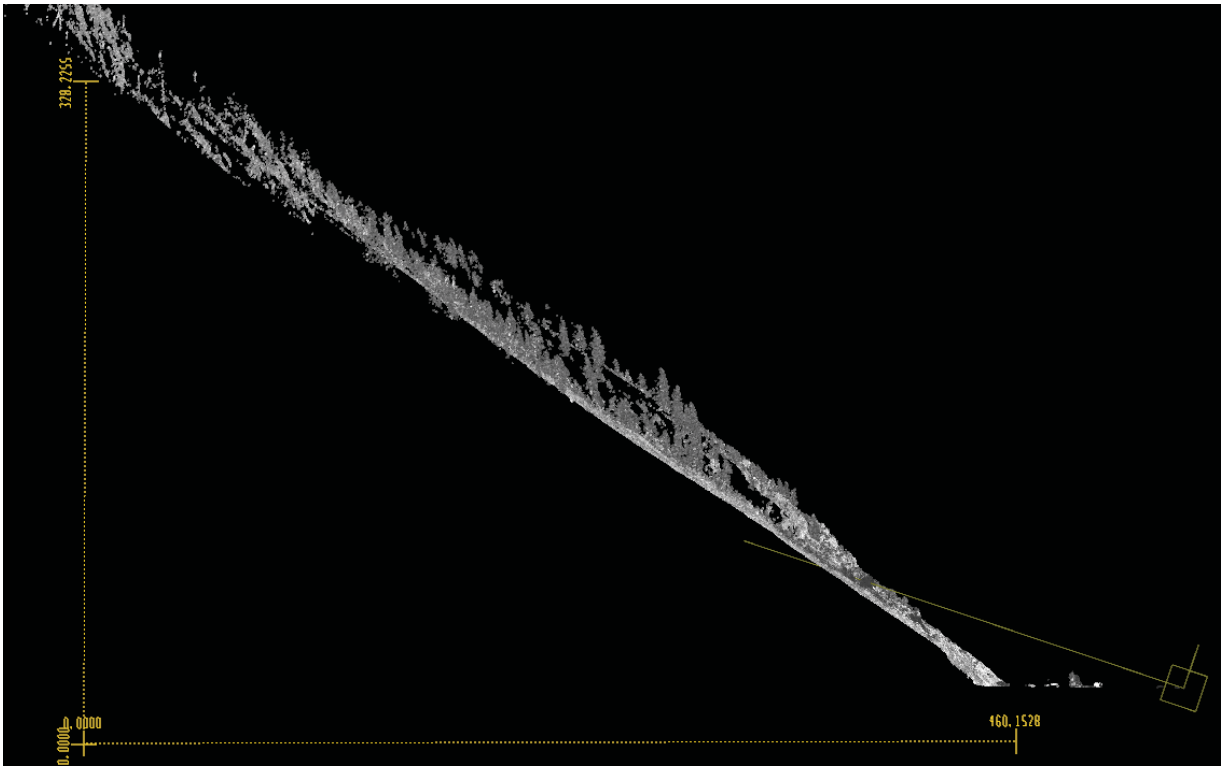

Figure 17b. Schematic. Side view of point cloud taken of site shown in Figure 17a.

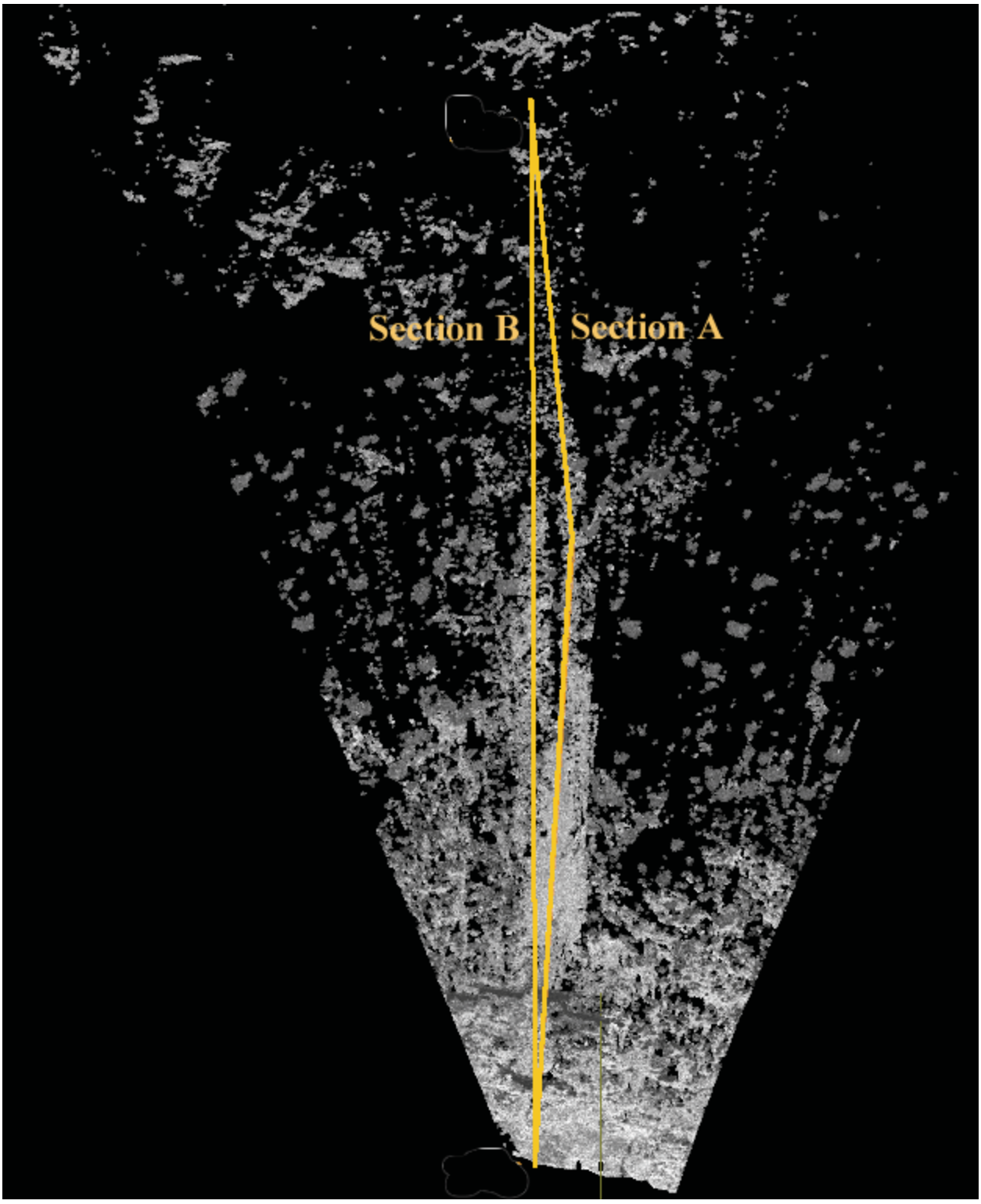

Figure 17c. Schematic. Plan view of point cloud showing the location of two cross sections.

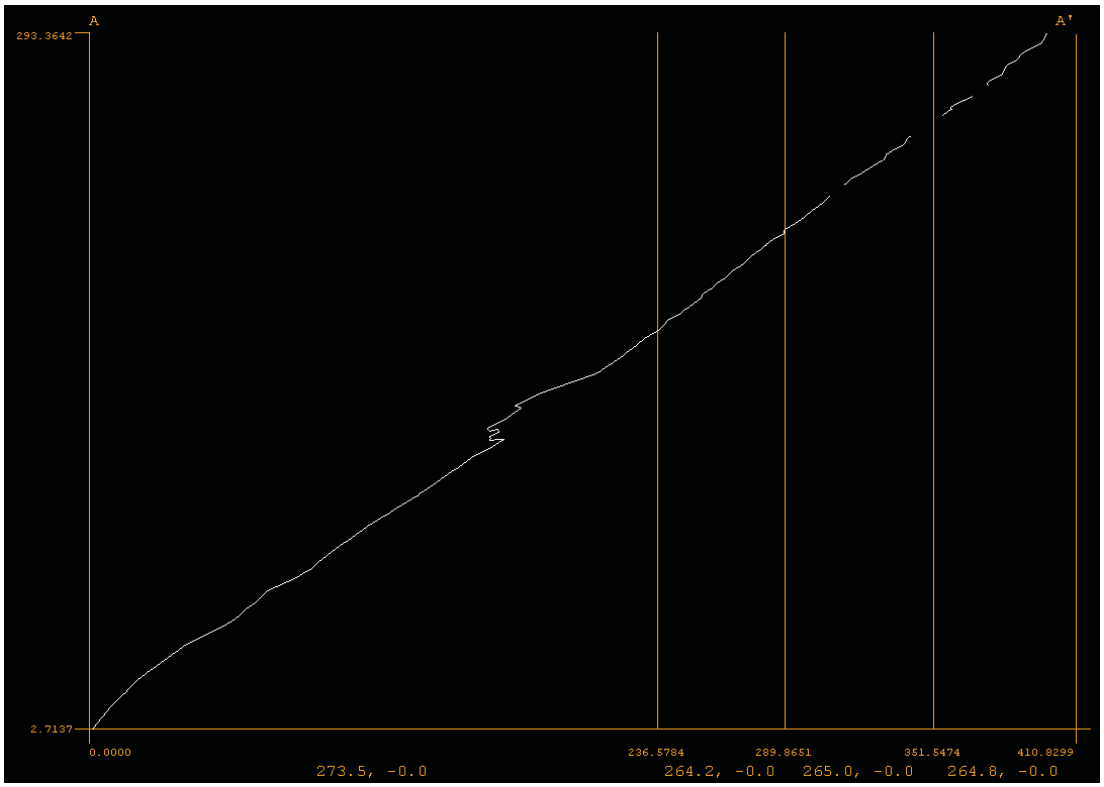

Figure 17d. Schematic. Section A (refer to Figure 17c).

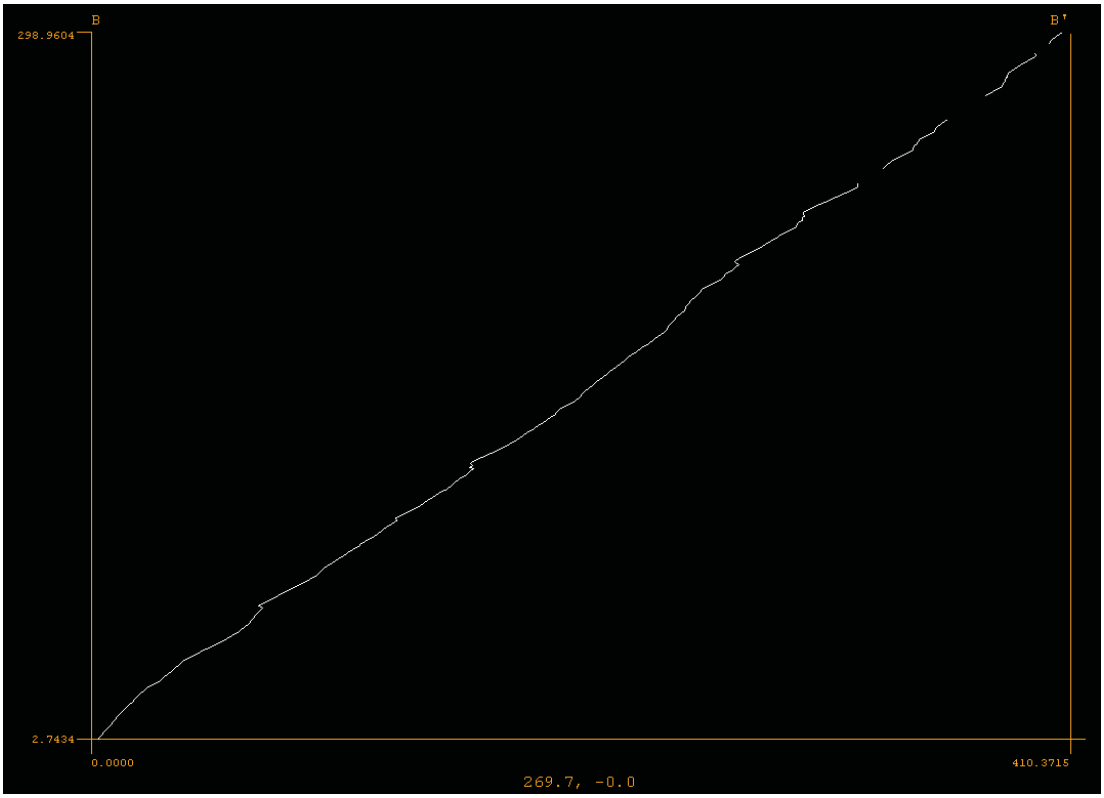

Figure 17e. Schematic. Section B (refer to Figure 17c).

Figure 17f. Photo. Close-up photo of center section of chute.

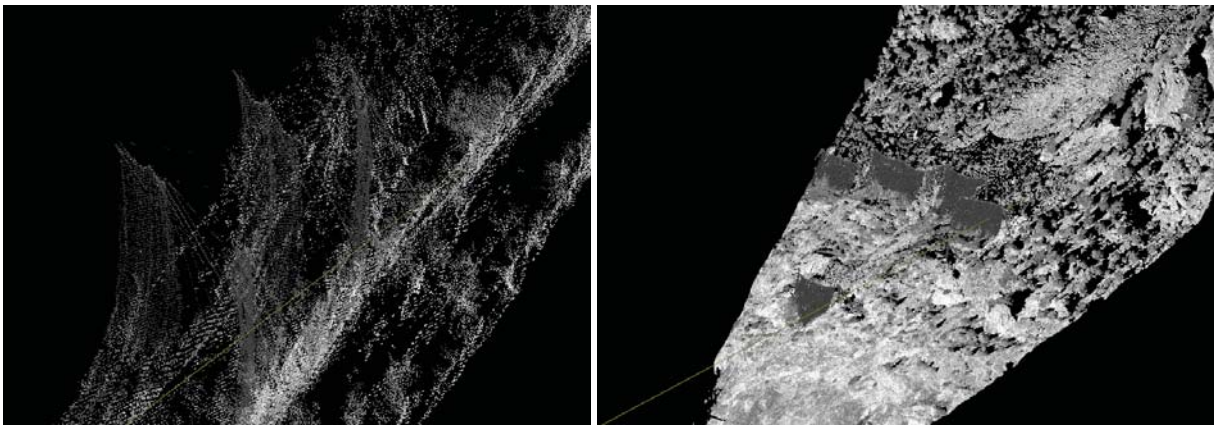

Figure 17g. Schematics. Close up views of point cloud showing rockfall fences.

Often a rock block does not travel to its final resting place once it dislodges from the source area. Rock blocks may slowly travel down a chute in a time-dependent fashion (during periods of rainfall, for example). Figure 18 is a photo of a small chute above Interstate 70 near Georgetown, Colorado (source area at the very top of the photo, Interstate 70 at the bottom of photo). It clearly shows several large blocks that have dislodged from the source area and are presumably moving down the slope in a time-dependent fashion. Rockfall monitoring with LiDAR can be used to understand this behavior, by taking scans at the same location but at

different times (every 6 months or every month, for instance). Rockfall monitoring with LiDAR is discussed in more detail in the next section.

Figure 18. Photo. Slope above the north side of Interstate 70 near Georgetown showing a small rockfall chute containing several large rock blocks.

Rockfall Monitoring

A very important application of LiDAR is rockfall monitoring. Rockfall monitoring is conducted by taking LiDAR scans of the same scene at some interval of time, say once every six months (or more often in areas with high rockfall risk). Figure 19 shows a LiDAR rockfall monitoring site on Interstate 70 near Georgetown, Colorado. The top part of the figure shows mapping that was conducted by the Colorado Dept. of Transportation of rock fall source areas and rockfall chutes (CDOT, 2005). The highest risk rockfall source areas are striped areas shown in red and lesser risk areas are striped areas in yellow and orange. The chutes are shown in purple. Interstate 70 goes through the middle of the photo and the town of Georgetown is the right of the photo. Permanent benchmarks have been set up along the bike path next to the interstate, as shown in the lower right photo of Figure 19. In total there are 20 benchmarks covering about 3 km (1.9 m) of Interstate 70.

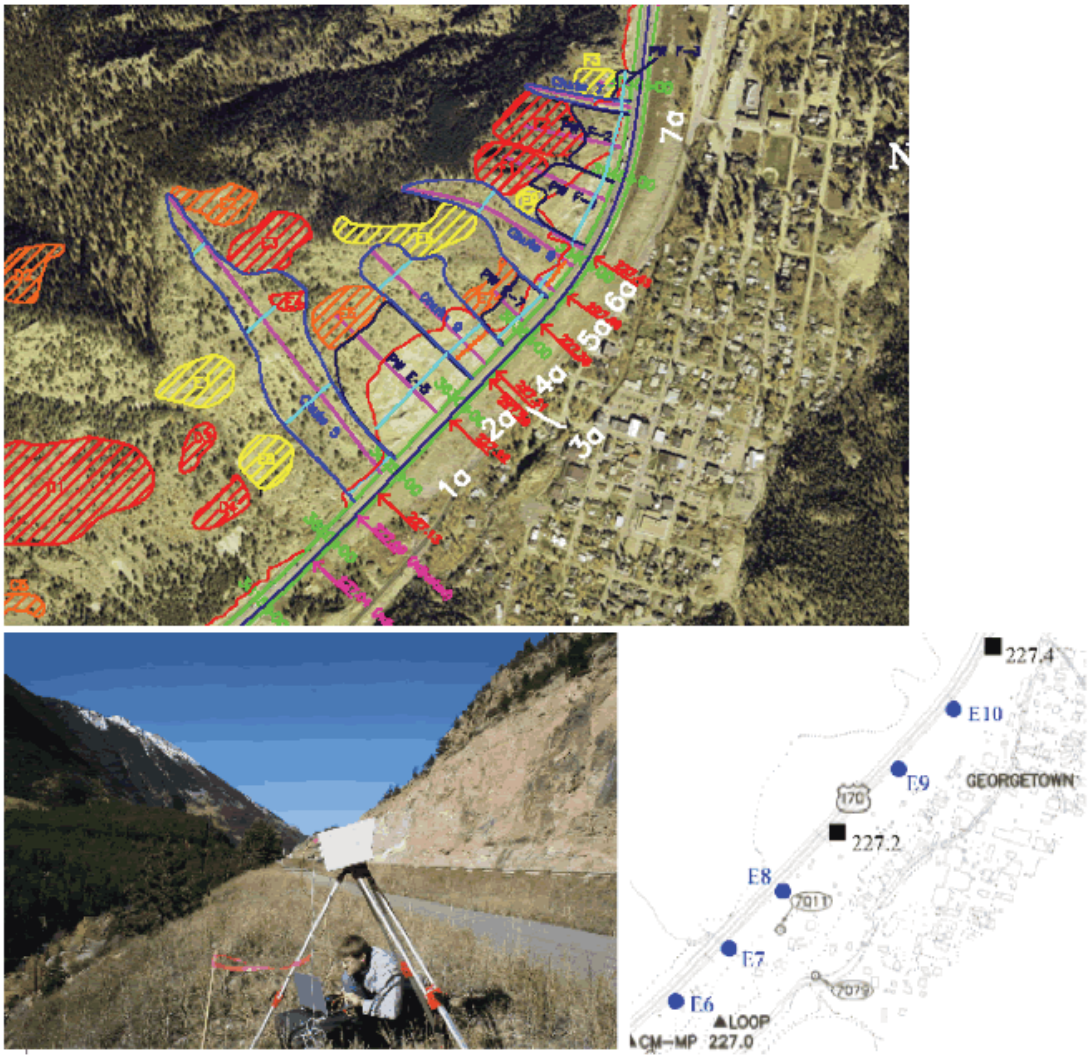

Figure 19. Photos and Schematic. Rockfall study area along Interstate 70 near Georgetown, Colorado. Top photo shows rockfall source and chute characterization, from CDOT (2007). Lower photo shows permanent benchmarks set up along bike path.

The periodic scans are processed to evaluate rockfall using "change algorithms". Change algorithms can be found in a number of the point cloud processing software. The change algorithms subtract two point clouds and produce a "difference cloud", which is a point cloud providing information on the relative difference between the two scans at points throughout the area that was scanned. From the change, the movement of a rock block can be tracked, or the size of a block that has move can be monitored. The total accumulated rockfall rate can also be calculated. Before the change algorithm can be applied, the two point clouds must be aligned as accurately as possible. In general, Iterative Closest Point (ICP) algorithms (Besl, 1992) are used to align the scans with the highest accuracy (higher than can be achieved by surveying alone).

A field site for testing change algorithms was set up at Milepost 2, Mt. Lemmon Highway, Arizona. A "rolling rock" experiment was conducted where 8 boulders with sizes from 10 to 100 cm were moved, as shown by the red circles in Figure 20a (larger circles represent larger boulders). Before and after scans were taken. The Iterative Closest Point (ICP) algorithm was applied and a difference point cloud was produced, as shown in Figure 20b. In Figure 20b, red indicates negative change (missing material compared with original scan), blue indicates positive change (new material). From this field site it was determined that the movement of boulders as small as 15 cm can be detected (the scans at this site were taken from a distance of about 60 m).

Figure 20a. Photo. Field site for testing change detection algorithms. Boulders marked with red circles were moved.

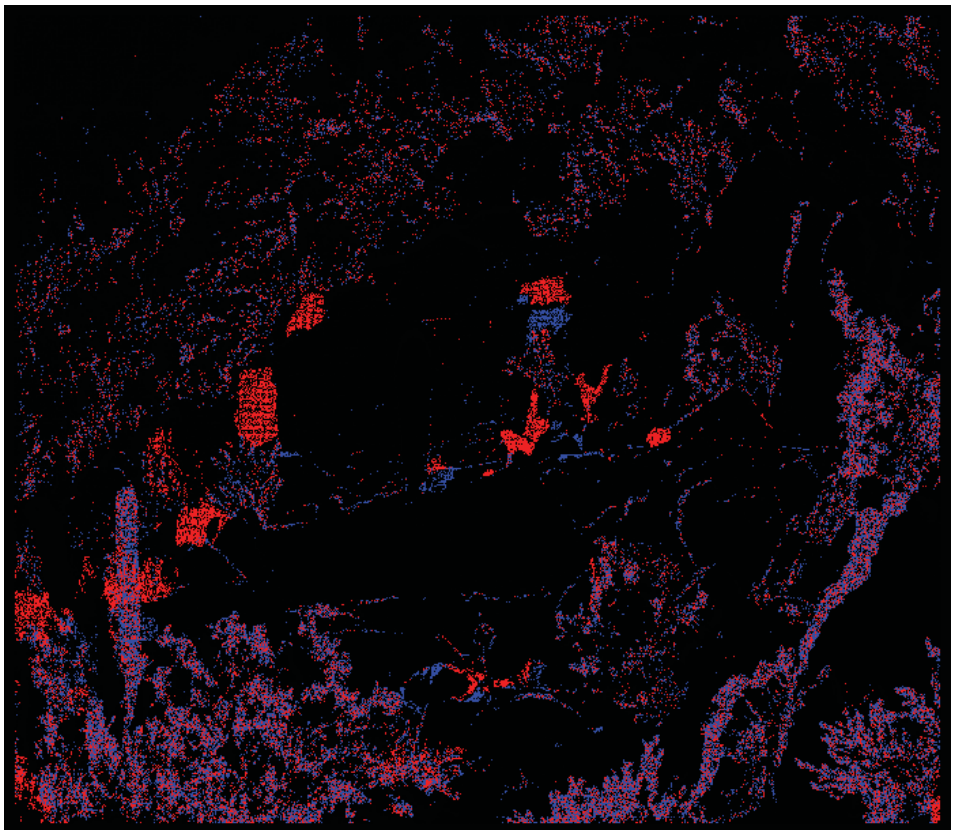

Figure 20b. Schematic. Difference point cloud. Red indicates negative change (missing material), blue indicates positive change (new material).

In addition to being used for safety purposes, the information from periodic scans can also be used to assist with rockfall maintenance. Figure 21 shows a rockfall fence filled with rock blocks. In order to work effectively, rockfall fences must be maintained, with a maintenance schedule dependent on the rockfall rate. Similar maintenance is required for rockfall ditches.

Figure 21. Photo. Rockfall Fence Containing an Overflow of Rock Fragments.

DETAILED 3D MEASUREMENTS

The last application of LiDAR for highway applications is the general area of detailed 3D measurements. LiDAR surveys provide a detailed "as built" that can be used for estimating various highway parameters, such as ditch width, slope height, roadway width, etc. These are parameters that are also used in estimating rockfall hazard ratings, as shown in Figure 22 (e.g., Patterson et al., 2002; Pack et al., 2002).

Before and after as-builts can also be used to verify the volume of a highway excavation, to accurately determine the shrink-swell behavior of particular rock type (Henwood et al., 2006), or to estimate stockpile volumes.

1. Slope height
2. Ditch effectiveness
3. Average vehicular risk
4. Sight distance
5. Roadway width
6. Structural condition (discontinuities)
7. Rock friction
8. Structural condition of eroded rock
9. Difference in erosion rates
10. Block size or volume of rockfall per event
11. Climate and presence of water on slope
12. Rockfall history.

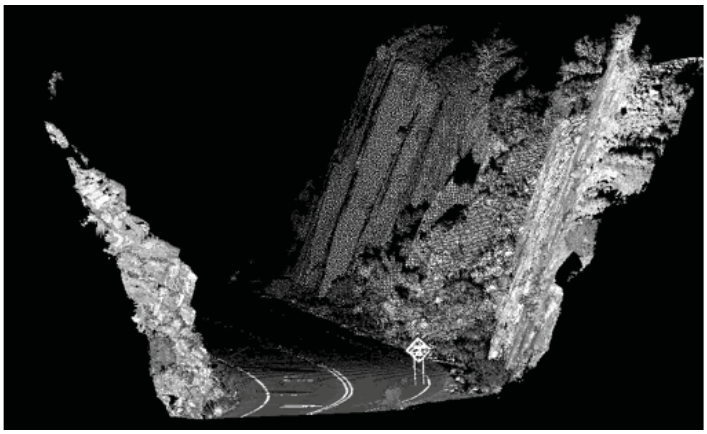

Figure 22. Schematic. Parameters used in many Rockfall Hazard Rating systems (left). Example of point cloud to estimate many of these parameters (right).